1 The SCBSD Algorithm

1.1 Motivation

Modeling 3D EM scattering from NS-NP is a challenging task; Conventional commercial softwares based on Finite Difference Time Domain (FDTD) or Finite Element (FEM) usually suffer difficulties when large field gradient or small radii of curvature are involved. The presence of small radii of curvature increases the computational effort, as it requires ultra-fine mesh and vast memory resources. Therefore, simulating complex geometry, with reliable results, is computationally expensive.

Several numerical methods have been proposed to overcome this problem, such as T-matrix method [1], Green's dyadic method with finite element [2] and discrete dipole approximation[3]. However, most of the commonly used techniques are either applicable to one type of geometrical configuration, require some sort of symmetry (*e.g.,* applicable to bodies of revolution), or their extension to complex 3D geometry is not trivial.

Here, we present a fast, accurate and robust calculation method for complex 3D NPs based on the SMT. Our method enables the calculation of the EM fields in and around 3D NPs with no rotational symmetry and with small radii of curvature, giving rise to deep investigation of the response of arbitrarily-shaped NPs to various EM fields.

In order to efficiently investigate 3D scattering by particles with arbitrary shape, we have developed a new algorithm which we termed Surface Curvature Based Source Distribution (SCBSD).

1.2 Sources' Distribution

The SCBSD algorithm takes into consideration the topology of the NP's surface and the number of sources used. It computes the local surface curvature, given by Gaussian Curvature (GC) or Mean Curvature (MC) [4], and distributes fictitious sources accordingly, thereby yielding appropriate expansion for the field distributions in and around the NP. Figure exemplifies how SCBSD algorithm is applied to arbitrary Non-Spherical (NS) objects. The red and blue stars are fictitious sources that approximate the EM fields inside and outside the surface, respectively. Areas with small radii of curvature require excessive proximity of the sources to the surface while the density of sources is determined by the variation rate of the surface curvature.

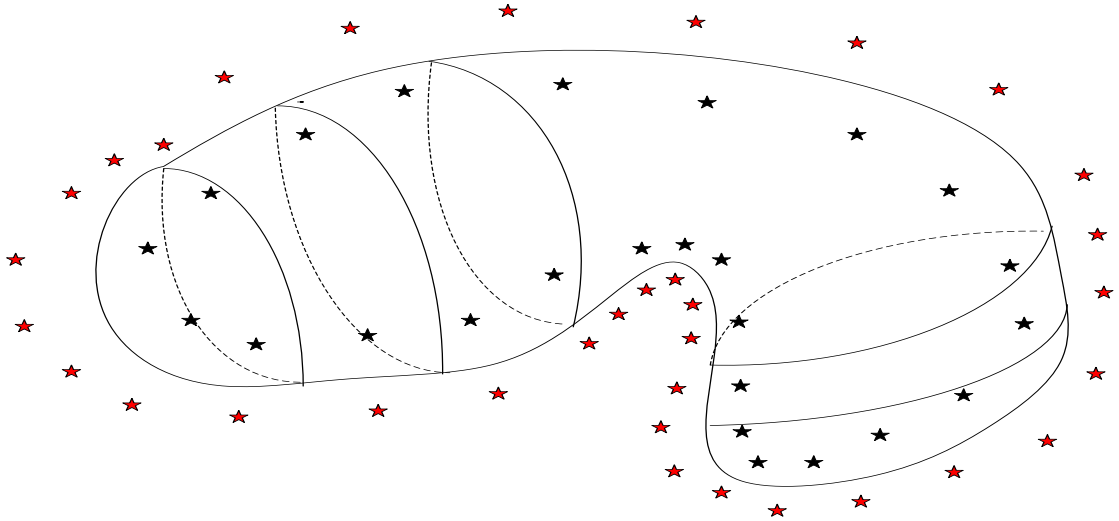

Figure 1. SCBSD Distribution of the sources for arbitrary surface

The choice of the 3D source surfaces (The mathematical surface on which the sources lie) and the layout of the sources over these surfaces can greatly affect the numerical solution accuracy. Good results, in terms of small *MBCE*, are mostly achieved by relating the sources' locations to a given geometry.

1.3 The Type of Sources

The types of sources are chosen to be multipole current sources, which are simple enough in complex 3D geometries. Figure depicts the distribution of multipoles inside arbitrary scatterer surface, which approximate the EM field outside the surface. Each multipole current density possesses locally the direction of tangential vector of the surface, but do not necessary lie on a small scale surface of the original. This choice of tangential multipoles enables every portion of the scatterer surface to be radiated by multipoles, with minimum overlap between their effective radiation zones. In the numerical aspect it minimizes the numerical dependence [5] between the sources, even though they are theoretically linearly independent as an expansion functions.

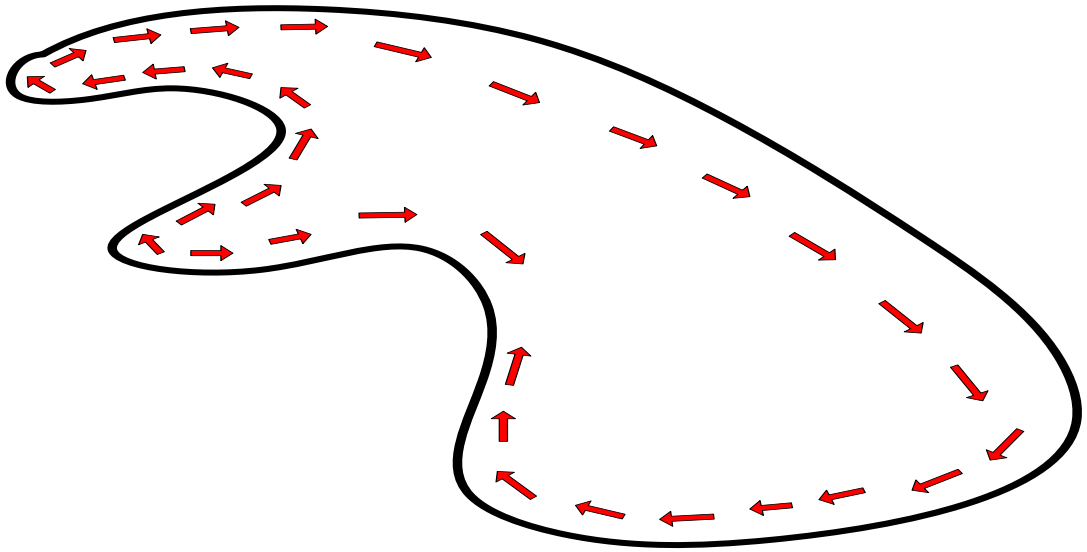

Figure 2. Usage of tangential multipoles in SCBSD algorithm for an arbitrary scatterer

Numerical considerations also impose limitations on the distance between the multipoles. On one hand, over adjacency of two neighbor sources might give rise to ill-conditioned impedance matrix and large *MBCE*, on the other hand, if adjacent multipoles are far enough from each other, one is more likely to get poor results as well, due to the absence of surface portions illumination. Therefore, there should be a compromise regarding the sources density and their closeness to the surface. The distance of multipoles to the surface should be less than wavelength λ, while the density depends on multipole order and on the distance from surface. Areas with small radii of curvature correspond to high order multipoles, owing to their ability to approximate the field in those areas with large field gradient. However, their associated fields are usually more complex and require additional computational

effort, whereas in areas with relatively large radii of curvature it is preferable to use more dipoles (zero order multipoles), whose fields are easier to calculate.

1.4 The Algorithm Step by Step

We now describe in detail our algorithm for a single scatterer given parametrically by $S = S(u,v)$. The SCBSD algorithm is composed of three steps which incorporate GMT rules [5] in locating multipoles and the concept of packing number which is explained in Ref [6].

Step 1:

The first step of the algorithm is to create from S the mathematical surface of the sources $S^s = S^s(u,v)$. We compute at each point on the surface S the mean radius curvature

$$\rho = \left(\frac{\kappa_1 + \kappa_2}{2} \right)^{-1} \tag{1}$$

where κ_1, κ_2 are the local principal curvatures (See Appendix). Each point on S_s is determined by a points on S, P_s, ρ and the wavelength λ in such a way that the distance between a point on S_s and P_s is $\min(d_s/2, \lambda/2, \rho/2)$, where d_s is the minimal distance between P_s and a point on the curve created by the intersection of S and a cross section of S which contain the normal to S at P_s.

Step 2:

In the second step we locate the sources along closed constant u and v curves. At first, the locations are evenly spaced along the curves. Hereafter, at each point we calculate the radius of curvature of the curve

$$G = \frac{|\gamma'|^3}{\sqrt{|\gamma'|^2 |\gamma''|^2 - (\gamma' \cdot \gamma'')^2}} \tag{2}$$

while between each two consecutive points , we choose the point of minimum G and add another source location in accordance with the normalized variation rate of G ,

$$V_G = \left| \frac{\partial G(l)}{\partial l} \right| / Max(G(l)) \tag{3}$$

where l denotes either u or v.

Step 3:

We choose the type sources in final step of the algorithm. Specifically, in each point source, which was set in previous step, we place two crossed-polarized multipoles, *i.e.*,

$$h_n^{(2)}\left(\left|\vec{r}-\vec{r}_s\right|\right)P_n^m\left(\cos\theta\right)e^{jn\phi}\hat{u}\ ,\quad h_n^{(2)}\left(\left|\vec{r}-\vec{r}_s\right|\right)P_n^m\left(\cos\theta\right)e^{jn\phi}\hat{v} \tag{4}$$

with $\hat{u},\hat{v}$ unit vectors tangent to S, $\vec{r}_s$ the point source and θ,ϕ the angles measured from $\vec{r}_s$. The order of multipoles (n,m) is determined by the curvature of S, namely, high order tangential multipoles are placed in areas with small radii, while low order multipoles should be located near low radii of curvature areas, due to their relatively simple EM fields.

Excessive adjacency of two consecutive multipoles imposes limitation on the number of sources along each closed curve, as it could either lead to poor results or impair the convergence test. Our experience has shown that keeping the distance s between two neighbor multipoles in the interval $0.1\left|G(u,v)\right| \le s < \lambda$ provides good results (MBCE $<$ 3%) in most scattering problems.

2 SMT vs Boundary Element Method

The main purpose of this section is to briefly compare our proposed SMT & SCBSD with the Boundary Element Method (BEM) in terms of speed, accuracy and complexity of implementation. Both SMT and BEM are integral methods and belong to the Method of Moments (MOM) class of techniques. While both methods have been proven to be very efficient in solving various complex electromagnetic problems, to determine which technique is more efficient depends very much on the specific properties of the problems to be solved. In terms of speed, SMT is considered to be a modification to BEM-like methods, by the virtue of using much lesser basis functions to approximate the fields. However, SMT has inherent problem with the location of the sources, which greatly affects the solution accuracy. This has been partially solved by our new SCBSD algorithm. In order to compare these methods, a simple case of illuminating Ag spheroid by a plane wave at a wavelength of $700nm$ (See Figure 3). The axes of the spheroid are $a=\frac{\lambda}{3}, b=c=\frac{\lambda}{12}$. This choice of axes constitutes a surface with very small radii of curvature ($<\frac{\lambda}{100}$), which raise great difficulty in achieving fast and accurate results.

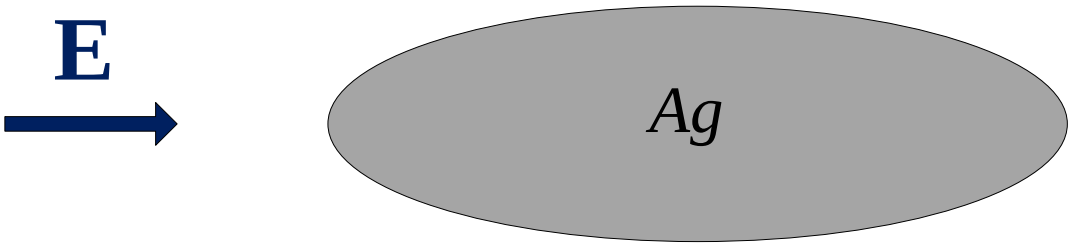

Figure 3. Plane wave excitation of a silver spheroid. The electric field is polarized along the major axis.

We employed the Integral Equation Solver of MWS-CST in order to provide results of the BEM. This solution was compared to SMT & SCBSD solution. Figure 4(a-b) depicts the relative boundary condition error of the four electromagnetic tangential components on spheroid surface in z=0 plane achieved by SMT and BEM, respectively.

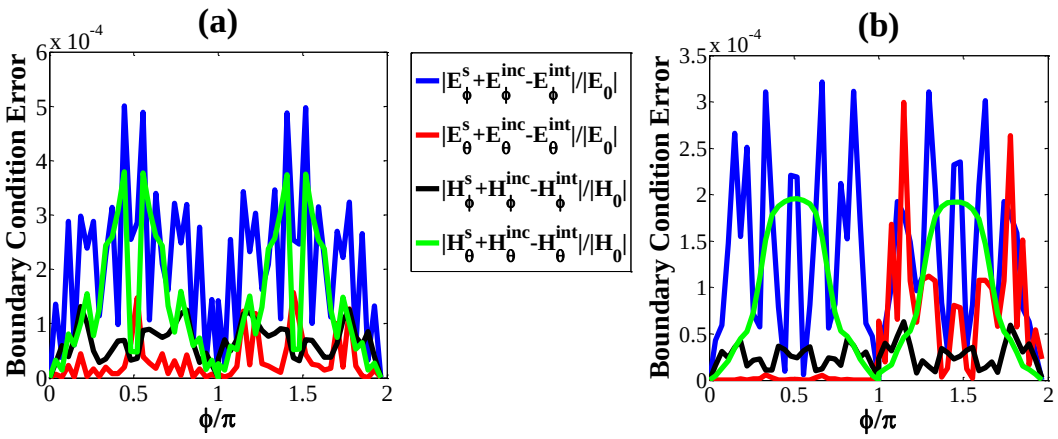

Figure 4. Boundary Condition Error in the continuity of tangential electromagnetic components, for BEM and SMT. The error was calculated in Z=0 plane along the longest contour. (a) BEM (b) SMT &SCBSD

Evidently, both methods yielded good results with Maximal Boundary Condition Error (MBCE) less than 0.05%. Both solutions also converged to the same solution, in terms of electric energy (relative error less than 0.1%).

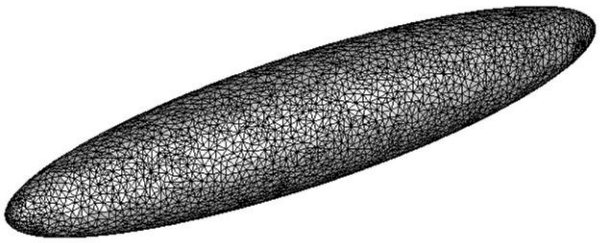

Figure 5. CST parameterization of ellipsoid. Areas of small radii of curvature are refined.

However, the BEM calculations for this case have been computationally demanding, namely it took 88 minutes (per wavelength) to plot these results on a super computer (4 CPUs, 115.2 GFLOPS each), while SMT required computation time 8.5 minutes on mild-level PC (28 GFLOPs). The computational burden, due to the complex parameterization of the automatic CST solver (Figure 5), was not encountered in SMT which generated relatively small matrices (typically 200x200). Table 1 summarizes the results.

Table 1. Comparison of the performance of BEM and SMT for scattering by plasmonic spheroid. BEM calculations were performed on High-level computer with 4 CPUs of 115.2 GFLOPS while SMT results were achieved on relatively Mid-level PC of 28 GFLOPs.

Method	CPU time (minutes)	MBCE (%)	Computer
Boundary Element Method (BEM)	88	< 0.05	High-level
SMT & SCBSD	8.5	<0. 035	Mid-level
SMT & SCBSD	1.5	0.65	Mid-level

The maximal boundary condition error (MBCE) in both cases was negligible ($< 0.035\%$), however the calculations of BEM approach, which were performed on super computer, consumed expensive computation time, almost hour and a half. SMT, on the other hand, yielded extremely fast results, including different electric field distributions as depicted in Figure 6 and 7.

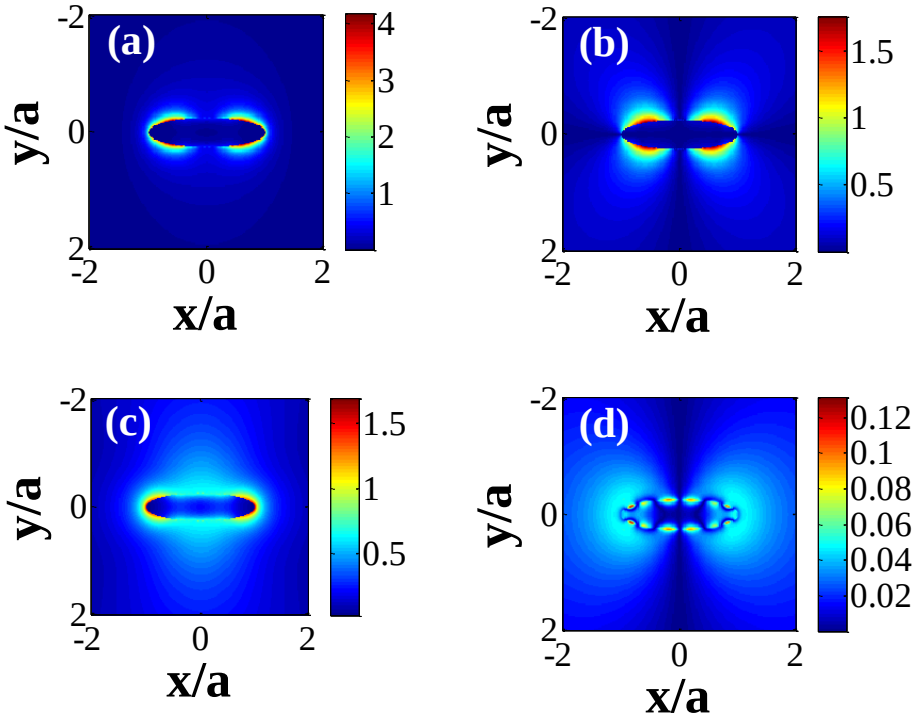

Figure 6. Different electric field distributions in z=0 plane generated by SMT. (a) Electric intensity, $|E|^2/|E_0|^2$ (b) y component, $|E_y|/|E_0|$ (c) x component, $|E_x|/|E_0|$ (d) z component, $|E_z|/|E_0|$

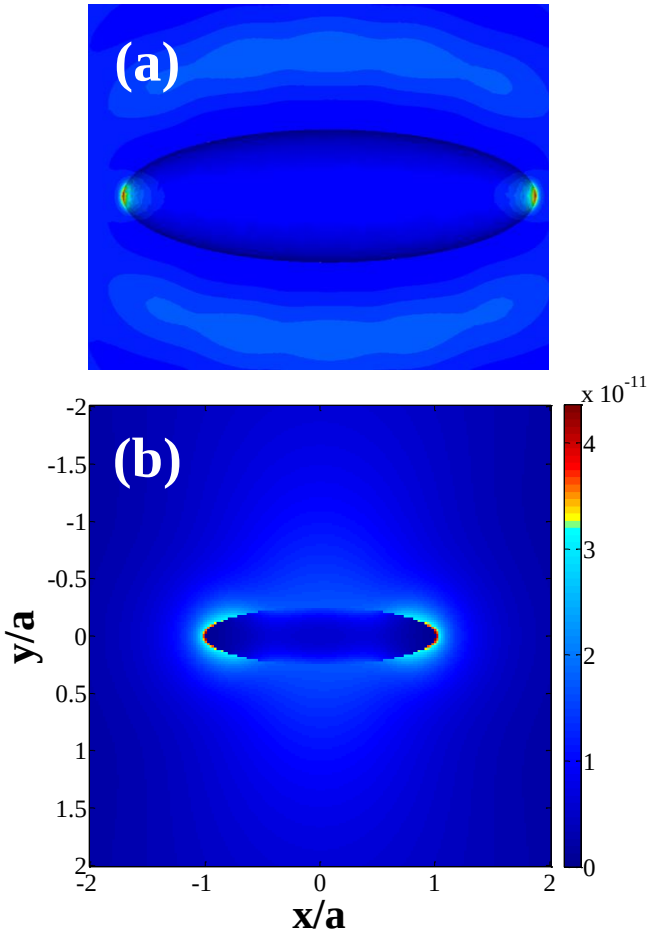

Figure 7. Electric energy distribution $\left[J / m^3 \right]$ in z=0 plane, as generated by both method. (a) CST (b) SMT.

Conclusions

Boundary Element Method attempts to use the given boundary conditions to fit boundary values into the integral equation, rather than values throughout the space defined by a partial differential equation. Like SMT, BEM solution, for a given problem, is achieved by solving an equivalent problem by matching the boundary conditions. The main difference is that in BEM the basis functions, which approximate the given solution, lie on the surface and are the boundary elements. It results in substantially larger matrices to compute as compared to SMT whose basis functions are placed at distance away from the boundary. Furthermore, BEM usually approximates 2D boundary of 3D problem by flat boundary elements such as triangles, which leads to sharp corners and edges, that is, locations where the first order derivative is discontinuous. Theoretically, field singularities are caused at these locations when certain materials are placed along the boundary and consequently, the numerical solution may not converge towards the analytical solution. More sophisticated elements or boundary discretization method would require additional computational effort. SMT circumvents this situation by approximating the boundary fields by smooth functions, thus avoiding the singularity issue [7] . Indeed, the fields' singularities have raised several difficulties with on-surface methods such as BEM and are also specified in ref [8]. Yet, while BEM-like methods can be easily extended to large and complex geometries, whereas the extension of SMT to different geometries is not trivial, as solution accuracy is very sensitive to sources location. The main advantage of SMT over BEM is the speed of calculations for complex geometries, which is considerably higher. Hence, owing to this merit, SMT is more suitable for investigating relations between the geometry to different electromagnetic parameters.

3 Cashew Nut & Peanut-Shell Particles Surfaces Parameterizations

Peanut-Shell Surface

$$x = R\left(\cos\phi^2 + 1/4\right)\cos\phi\sin\theta$$
$$y = R\left(\cos\phi^2 + 1/4\right)\sin\phi\sin\theta$$
$$z = R\cos\theta$$

Cashew Nut Surface

The cashew-nut function g is a function of $g = g(z,\phi,b,d)$, where b,d are free parameters which determined the inner diameter (concave region) and the dimensions of the cashew along z direction, respectively.

$$c \triangleq 1/(2b)$$
$$a_1(z) \triangleq b - z^2(b-c)/2$$
$$a_2(z) \triangleq c + z^2(b-c)/2$$
$$r_1(z) \triangleq \left(a_1(z) - a_2(z)\right)/2$$

$$m_1(z) \triangleq \left(a_1(z) + a_2(z)\right)/2$$
$$m_2(z) \triangleq 3a_2(z)/2 - a_1(z)/2$$

$$\begin{aligned} x &= a_1(z)\cos\phi \\ y &= a_1(z)\sin\phi \\ z &= d\sin(\pi z/2) \\ \phi &\in [0,\pi] \end{aligned}$$

$$f_1(z) = e^{-1000(\varphi-\pi)^2}$$

$$f_2(z) = e^{-1000(\varphi-2\pi)^2}$$

$$r_2(z) = m_1(z)\, f_1(z) + r_1(z) + m_2(z)\, f_2(z)$$

$$\begin{aligned} x &= -m_1(z)/2 + r_1(z)\cos\phi \\ y &= r_2(z)\sin\phi \\ z &= d\sin\left(\pi z/2\right) \\ \phi &\in [\pi, 2\pi] \end{aligned}$$

$$\begin{aligned} x &= -a_2(z)\cos\phi \\ y &= a_2(z)\sin\phi \\ z &= d\sin\left(\pi z/2\right) \\ \phi &\in [2\pi, 3\pi] \end{aligned}$$

$$f_3(z) = e^{-1000(\varphi-3\pi)^2}$$

$$f_4(z) = e^{-1000(\varphi-4\pi)^2}$$

$$r_3(z) = m_2(z)\, f_3(z) + r_1(z) + m_1(z)\, f_4(z)$$

$$\begin{aligned} x &= m_1(z)/2 + r_1(z)\cos\phi \\ y &= r_3(z)\sin\phi \\ z &= d\sin\left(\pi z/2\right) \\ \phi &\in [3\pi, 4\pi] \end{aligned}$$

References

[1] T. Wriedt, "A review of elastic light scattering theories," *Part.Syst.Charcat,* vol. 15, pp. 67-74, 1998.

[2] J. P. K. a. O. J. F. Martin, "Accurate solution of the volume integral equation for high-permittivity scatterers," *IEEE Trans. Antennas Propa,* vol. 48, pp. 1719-1726, 2000.

[3] H. DeVoe., "Optical properties of molecular aggregates. I. Classical model of electronic absorption and refraction," *J. Chem. Phys,* vol. 41, p. J. Chem. Phys, 1964.

[4] W. A. M. S. Kühnel, Differential Geometry: Curves - Surfaces - Manifold, American Mathematical Society, 2006.

[5] C. Hafner, The Generalized Multipole Technique for Computational Electromagnetics, Boston: Artech House, 1990.

[6] K. I. B. a. J. E. Richie, "On the location and number of expansion centers for the generelized multiple technique," *IEEE Trans.Electromagnetic Compatibility* , vol. 38, pp. 177-180, 1996.

[7] Y. L. a. A. B. a. A. Boag., "Generalized formulations for electromagnetic scattering from perfectly conducting and homogeneous material bodies-theory and numerical solution.," *Antennas and Propagation, IEEE,* vol. 36, no. 12, pp. 1722-1734, 1988.

[8] A. L. Y. &. W. J. K. hochman, "On the use of rational-function fitting methods for the solution of 2D Laplace boundary-value problems," *Journal of Computational Physics,* vol. 238, pp. 337-358, 2013.